Journal of Alloys and Compounds 509 (2011) 9010–9014

Contents lists available at ScienceDirect

Journal of Alloys and Compounds

journal homepage: www.elsevier.com/locate/jallcom

Electrochemical performances of Co-doped $LiFePO_4$/C obtained by hydrothermal method

Jueming Yang, Ying Bai, Chunbo Qing, Weifeng Zhang*

Key Laboratory of Photovoltaic Materials of Henan Province and School of Physics and Electronics, Henan University, Kaifeng 475004, PR China

A R T I C L E   I N F O

Article history:
Received 2 April 2011
Received in revised form 17 June 2011
Accepted 9 July 2011
Available online 19 July 2011

Keywords:
Lithium iron phosphate
Carbon coating
Cobalt doping
Hydrothermal method
Lithium ion batteries

A B S T R A C T

$LiFePO_4$, C-coated $LiFePO_4$ ($LiFePO_4$/C), and Co-doped $LiFePO_4$/C as cathode materials for lithium ion batteries are synthesized by a hydrothermal method. The electrochemical properties of the three samples are investigated and compared by galvanostatic cycling, rate capability and cyclic voltammetry (CV) measurements. $LiFePO_4$, $LiFePO_4$/C, and Co-doped $LiFePO_4$/C exhibit initial discharge capacities of 88, 90 and 116 mAh g^{-1} at 0.1 C, respectively. After annealing at 400 °C, the initial discharge capacities of the three corresponding samples increase to 115, 125 and 132 mAh g^{-1} at 0.1 C. In both cases, Co-doped $LiFePO_4$/C shows the best rate performance among the three samples. CV measurements indicate that the improvement of dynamic behavior could be attributed to Co doping. All experimental observations indicate that the preparation of Co-doped $LiFePO_4$/C offers a way to combine the common methods to improve the performance of $LiFePO_4$: particle size reduction, intimate conducting phase coating and metal supervalent doping, which explain the enhanced electrochemical properties.

1. Introduction

Electric vehicles and hybrid electric vehicles are two kinds of future transportation tools to substitute the traditional petrol vehicles, and yet power cell has become a bottleneck and blocked their widespread applications. In recent years, great efforts have been paid to develop lithium ion batteries with excellent thermal stability, high energy and power density. Since the pioneering work of Goodenough and coworkers [1], $LiFePO_4$ has attracted increasing great interest all over the world for its many advantages such as high theoretical capacity (170 mAh g^{-1}), low cost, and high compatibility with environment. In fact, it has been recognized as one of the most promising candidates to replace lithium cobalt oxide as the cathode material for lithium ion batteries. However, the drawbacks of $LiFePO_4$ mainly lie in low electronic conductivity and slow diffusion of Li^+ ions, resulting in fast capacity decay, especially under high current densities [1,2], which has greatly inhibited its large-scale application [3]. Recently, great improvements have been achieved in the performance of $LiFePO_4$, with the methods mainly focusing on particle size reduction [4–8], intimate conducting phase coating [9,10], and metal supervalent doping [11–15].

Hydrothermal synthesis has been proven a successful method to prepare $LiFePO_4$ with small particle size for its many merits, such as easy to produce, economical in energy and easily scalable, etc. [16–23]. However, this method is apt to produce $LiFePO_4$ with low order of crystallinity and iron occupational disorder [24], which may affect the diffusing channels of Li^+ ions. Thus the specific capacity of $LiFePO_4$ synthesized by hydrothermal method is rather low (about 85 mAh g^{-1} at 0.1 C) compared with that of solid state reaction (about 150 mAh g^{-1} at 0.1 C) [24]. To improve the electrochemical properties of $LiFePO_4$ with small particle size synthesized by hydrothermal method, as a feature of this work, the samples were prepared at a higher temperature to increase the order of crystallinity.

Very recently, La-doped $LiFePO_4$/C has attracted attention of only a few researchers [25], though this method has been proven to be very effective. In this paper, with the combination of general modification methods of carbon coating and Co doping, the hydrothermally prepared Co-doped $LiFePO_4$/C exhibits greatly improved electrochemical performance. The enhancement mechanism is preliminarily explored by CV measurements.

2. Experimental

2.1. Preparation of samples

$LiFePO_4$, C-coated $LiFePO_4$ ($LiFePO_4$/C) and Co-doped $LiFePO_4$/C were synthesized by a hydrothermal method. For simplicity, the samples of $LiFePO_4$, $LiFePO_4$/C and Co-doped $LiFePO_4$/C hereafter are named as LFP, LFP/C and CoLFP/C, respectively. The starting materials are $LiOH{\cdot}H_2O$ (95.0%, Zhengzhou Paini), $FeSO_4{\cdot}7H_2O$ (99.0%, Tianjin kermel), H_3PO_4 (85.0%, Tianjin kermel), $Co(CH_3CO_2)_2{\cdot}4H_2O$ (99.5%, Shanghai Hengxin) and sucrose (AR, Tianjin De'en). For LFP and LFP/C, the molar ratio of Li:Fe:P in the precursor solution is 3:1:1. The molar ratio of Li:Fe:P:Co is 3:0.9:1:0.1 for CoLFP/C. The concentrations of Fe^{2+} and sucrose in the reaction solution were controlled at 0.5 mol L^{-1} and 7 g L^{-1}, respectively. In the preparation

---

* Corresponding author. Tel.: +86 378 3880 696; fax: +86 378 3880 659.
E-mail addresses: wfzhang@henu.edu.cn, wfzhang6@163.com (W. Zhang).

0925-8388/$ – see front matter © 2011 Elsevier B.V. All rights reserved.
doi:10.1016/j.jallcom.2011.07.021

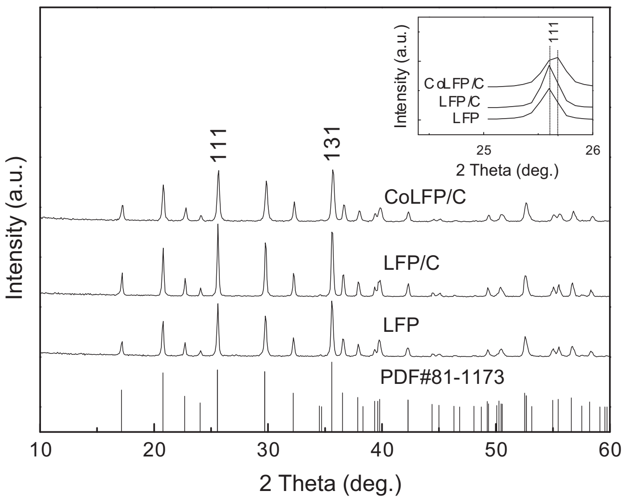

Fig. 1. XRD patterns of LFP, LFP/C and CoLFP/C.

process of pristine $LiFePO_4$, $LiOH{\cdot}H_2O$ and $FeSO_4{\cdot}7H_2O$ were separately dissolved in deionized water. Afterwards, H_3PO_4 was added into the $FeSO_4{\cdot}7H_2O$ solution to avoid the formation of $Fe(OH)_2$, Fe (II) in which is easily oxidized to Fe (III). Then, LiOH solution was added to the mixture dropwise through separatory funnel. The thoroughly dissolved solutions were mixed together homogeneously with fiercely stirring. The final mixture was swiftly transferred to a 0.1 L stainless steel autoclave and heated at 220 °C for 2 h. Finally, the light green precipitate was filtered and air-dried. LFP/C was prepared by adding sucrose to the $FeSO_4$ solution via the same process as LFP. For the preparation of CoLFP/C, $FeSO_4$ and sucrose solutions were mixed at first, and then $Co(CH_3CO_2)_2$ aqueous solution was added to this mixture drop by drop. The subsequent processes were the same with those of the LFP.

2.2. Structure and morphology characterization

X-ray diffraction (XRD) measurements were performed on a diffractometer (DX-2500, Fangyuan) with Cu K_α radiation with $\lambda = 1.54145$ Å. Raman spectra were collected on a laser Raman spectrometer (RM-1000, Renishaw) at $\lambda_0 = 457.5$ nm. The carbon contents of the synthesized LFP/C and CoLFP/C particles were determined by an elemental analyzer (PE2400-II, American). Morphologies of the as-prepared samples were examined using scanning electron microscopy (SEM, JSM-6390LV, Jeol) with acceleration voltage of 20 kV, a beam size of 20 nm, a beam current of 1×10^{-8} A, at $P_0 = 10^{-4}$ Pa.

2.3. Electrochemical characterization

The working electrodes were fabricated by compressing the mixtures of 70 wt.% active materials (the as-prepared three samples), 20 wt.% acetylene black (Super-P, MMM Carbon), and 10 wt.% binder (polyvinylidene fluoride, PVDF) dissolved in N-methyl-pyrrolidone (NMP) on a 20 μm thick aluminium foil. The casted aluminium foil was put into vacuum oven and heated at 120 °C for 12 h. Then the film was carefully cut into uniform square pieces with side length of 8 mm as the working electrode. The electrolyte was 1 M $LiPF_6$ dissolved in a mixture of ethylene carbonate (EC) and diethyl carbonate (DEC) with a volume ratio of 1:1. Celgard 2400 was used as the separator, and Li foil served as the counter electrode. The assembling process was conducted in an argon-filled glove box with H_2O and O_2 content less than 1 ppm. The galvanostatic cycling was measured on a Land cell test system (Land CT 2001A) between cut off voltages of 2.3 and 4.2 V (vs. Li/Li$^+$). Cyclic voltammetry (CV) was measured in a three electrode system using electrochemical workstation (CHI660C, Shanghai). The CV curves were recorded between 2.3 and 4.2 V at a scan rate of 0.1 mV s^{-1}.

3. Results and discussion

3.1. Physical characterizations

The XRD patterns of LFP, LFP/C and CoLFP/C are displayed in Fig. 1. All samples exhibit well-defined olivine structures, belonging to space group orthorhombic *Pnmb*. No diffraction peak from impurity can be recognized in the three patterns. $R = I_{(1\,1\,1)}/I_{(1\,3\,1)}$ is defined as the intensity ratio of the (1 1 1) to the (1 3 1) peaks, which is used to estimating the degree of cation order in olivine-type materials. Generally, the electrochemical properties can be improved with the enhancement of degree of cation order [26]. In the present work, the calculated values R are 0.7633, 0.8705 and 0.8853 for LFP, LFP/C and CoLFP/C. Among the three samples, CoLFP/C shows the highest degree of cation order, which can be confirmed by the electrochemical results afterwards. The inset in Fig. 1 is the selected XRD patterns of the three as-prepared samples over a 2θ range from 25° to 26°, from which it can be clearly observed that the (1 1 1) diffraction peak shifts towards higher angle for CoLFP/C.

Table 1
Lattice constants of LFP, LFP/C and CoLFP/C.

a (Å)	*b* (Å)	*c* (Å)
PDF 81-1173		
6.010	10.332	4.692
LFP		
5.984(8)	10.321(4)	4.692(9)
LFP/C		
5.985(1)	10.312(7)	4.689(8)
CoLFP/C		
5.960(9)	10.295(4)	4.685(4)

The calculated lattice constants of the as-prepared samples are listed in Table 1. The lattice parameters of LFP/C changed little compared with those of LFP, indicating that the coated carbon layers can only influence the surface of $LiFePO_4$ particles and almost have no effect on the bulk. The lattice constants of CoLFP/C decrease prominently, which agrees well with the XRD curve shift (inset in Fig. 1). These results imply that the Fe^{2+} ions have been partly substituted by Co^{2+} ions, since the ionic radius of Co^{2+} (0.74 Å) is slightly smaller than that of Fe^{2+} (0.76 Å) [12]. Calculation by Scherrer equation demonstrated that the grain sizes of LFP, LFP/C and CoLFP/C are similar (about 26 nm).

Raman spectroscopy is a powerful analytical tool for probing the structural properties of electrode materials, which is quite suitable for detecting phosphate-based cathodes, as the intramolecular vibrational modes of the $PO_4{}^{3-}$ anions produce rich and intense bands in Raman spectra. Therefore, it can be applied to further identify the surface structure of the as-prepared samples. The Raman spectra of the three as-prepared samples are plotted in Fig. 2, from which no modes belonging to impurities can be identified. Common features can be observed below 1200 cm^{-1}, which are the characteristic vibrations of $LiFePO_4$ lattice. The sharp bands at 1068, 998 and 952 cm^{-1} can be attributed to the intramolecular stretching motions of $PO_4{}^{3-}$ [27]. The bands around 1600 and 1330 cm^{-1} (very weak) are very well known and ascribable to the presence of the graphitic carbon (G-band) and the disordered carbon (D-band)

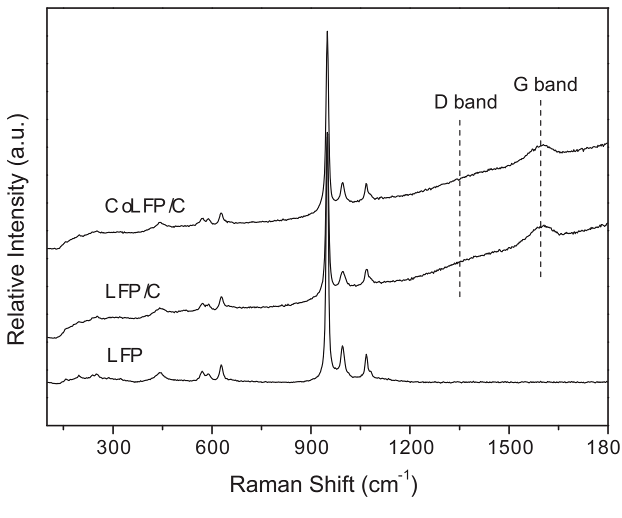

Fig. 2. Raman spectra of LFP, LFP/C and CoLFP/C.

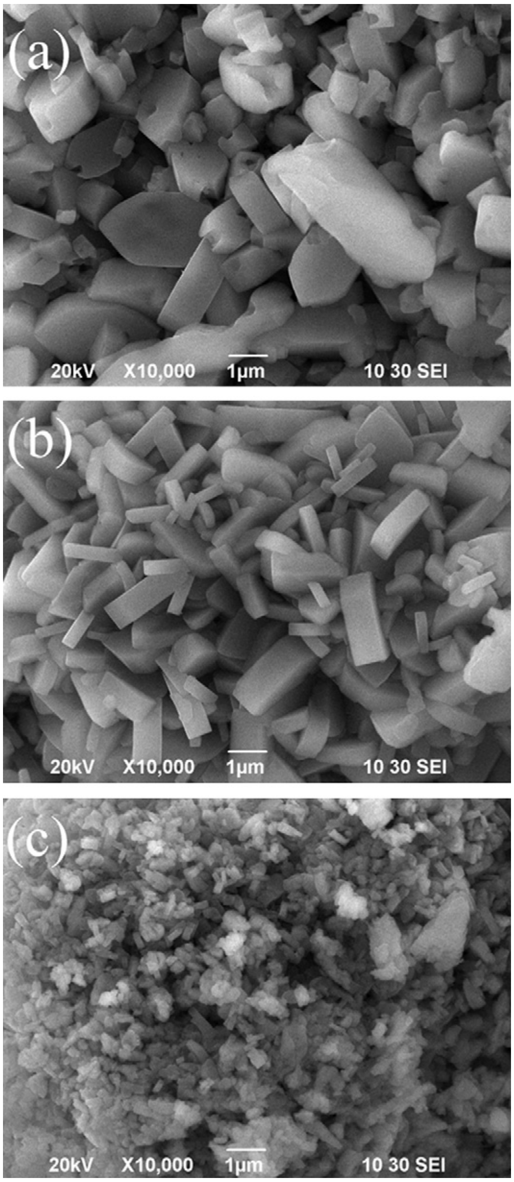

Fig. 3. SEM images of LFP (a), LFP/C (b) and CoLFP/C (c).

covering the triphylite particles [28]. The intensity ratio (I_D/I_G) indicates crystallinity of the coated carbon, for example, the smaller the ratio, the higher the order degree of the coated carbon layers [29]. In this work, the I_D/I_G ratios of carbon in LFP/C and CoLFP/C are very low, indicating high degree of carbon ordering in the two composite materials. As shown in Fig. 2, the coated carbon layers in this work are highly graphitized for LFP/C and CoLFP/C, which are expected to contribute to the enhancement of the electronic conductivity of the samples.

The carbon contents in LFP/C and CoLFP/C determined by the element analyzer are 0.35 wt.% and 0.34 wt.%, respectively. Though the coating contents of carbon are rather low in the two samples, Raman spectra demonstrated the existence of carbon in Fig. 2.

Fig. 3 illustrates the SEM images of the as-prepared LFP, LFP/C and CoLFP/C powders. The particles of LFP and LFP/C have the similar feature of plate-type morphologies with average thicknesses of 1000 and 500 nm. The plate-type shape is regarded as the typical morphology of phosphate related materials synthesized through a similar hydrothermal process [30]. As can be clearly seen from Fig. 3, the LFP/C particles are more homogeneously built up with more acute and regular edges compared with those of LFP, indicating that the particles grow more completely after carbon-coating. However, the morphology of CoLFP/C is greatly different from those of LFP and LFP/C (Fig. 3(c)), showing uniform fine particles with an average size of 200 nm. In general, the morphology of $LiFePO_4$ changes little after C-coating, while, it experiences great change after Co-doping. The markedly changed morphology of CoLFP/C provides another strong evidence of Co doping in $LiFePO_4$ lattice. The doped Co^{2+} ions will substitute Fe^{2+} ions and result in the formation of $LiFe_{1-x}Co_xPO_4$.

When the as-prepared samples were repeatedly washed with deionized water in the preparation process, there were plenty of suspended particles in the water. Among the three samples, it is most difficult for the suspended particles of CoLFP/C to deposit completely, indicating that the CoLFP/C particles are smaller than LFP and LFP/C, consisting with the SEM results. It is one of the important strategies to reduce the path length over which the electron and Li ion have to move by using nano-sized materials [31]. Considering the improved degree of cation order and the small particle size, the CoLFP/C sample is expected to exhibit enhanced electrochemical performances compared with LFP and LFP/C, which will be described in the following discussion.

3.2. Electrochemical characteristics

The initial charge–discharge profiles of the as-prepared samples of LFP, LFP/C and CoLFP/C are shown in Fig. 4(a). The stable charge–discharge plateaus are the characteristic of $LiFePO_4$ materials. The initial discharge capacities are 88, 90 and 116 mAh g^{-1} and the first cycle efficiencies are 89.4%, 89.6% and 95.6% at 0.1 C for the samples of LFP, LFP/C and CoLFP/C, respectively. Among the three samples, the charge–discharge plateaus of CoLFP/C are much more longer than those of LFP and LFP/C, implying higher initial capacities of this material. The direct carbon coating on the particle surface of $LiFePO_4$ introduced in the synthesis process will enhance the electronic conductivity and improve the sluggish kinetics behavior [7], which explains the enhanced electrochemical profile of LFP/C than LFP. However, only slight improvement has been obtained after carbon coating, as demonstrated in Fig. 4(a), which can be attributed to the rather low content of carbon coating (0.35 wt.%) in LFP/C.

Cycling behavior of the three samples is displayed in Fig. 4(b). The batteries were cycled between 2.3 and 4.2 V at 0.1 C. After 100 cycles, the discharge capacities decrease to 64, 71 and 96 mAh g^{-1}, with capacity retentions of 73%, 79% and 83%, respectively. No large improvement of cycling performance can be achieved after carbon-coating, showing the limitation of this conventional method. With the same content of coated carbon, CoLFP/C exhibits greatly increased specific capacity and improved capacity retention, implying the prominent influence of Co doping in this case.

The rate performances of the three samples are compared in Fig. 4(c). The electrodes were cycled at 0.1 C, 1 C, and 2 C between 2.3 and 4.2 V, respectively. For the sample of LFP, its specific capacity undergoes the fastest deterioration as the rate increases. Carbon coating is beneficial for the rate performance; however, only limited improvement can be achieved. The specific capacities of LFP and LFP/C remain only 17 and 30 mAh g^{-1} at 2 C rate at the 100th cycle. In comparison, CoLFP/C manifests the best rate performance. Its specific capacity remains nearly 80 mAh g^{-1} at 2 C and keeps almost unchanged from 30th to 100th cycles. After 200 cycles at 2 C, there still remains the specific capacity of 76 mAh g^{-1} for CoLFP/C (not shown in Fig. 4(c)). The discharge specific capacity falls only 3.8%, 3 mAh g^{-1}, from the 32nd to 200th cycles. All these results show that the electrochemical performances of carbon-coated $LiFePO_4$ have been greatly enhanced by Co doping.

It is a usual method to deal with hydrothermally synthesized $LiFePO_4$ by post annealing treatment [32]. After annealing, its crys-

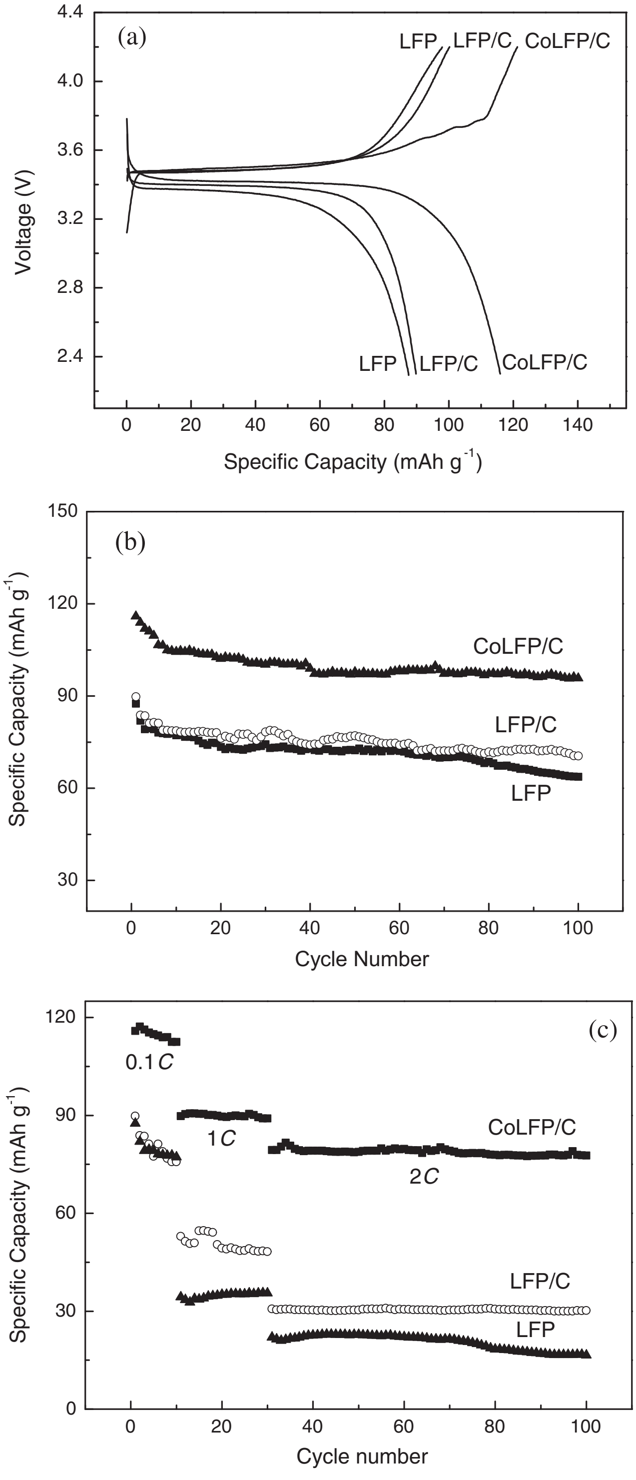

Fig. 4. The initial charge–discharge profiles at 0.1 C (a), cycling behaviors at 0.1 C (b) and comparison of rate performances (c) of LFP, LFP/C and CoLFP/C.

tallization as well as electrochemical properties can be improved. In the present work, the three as-prepared samples were annealed at 400 °C under the protection of argon and hydrogen mixture (hydrogen 5 wt.%) for 1 h.

Generally, the electrochemical performances of the three samples are obviously improved after annealing, as can be observed in Fig. 5(a). Fig. 5 exhibits the initial charge–discharge profiles of the three samples after annealing. At the rate of 0.1 C, the initial discharge specific capacities of annealed LFP, LFP/C and CoLFP/C are 115, 125 and 132 mAh g^{-1}, respectively. The specific capacity of annealed CoLFP/C experiences an activation process in the first several cycles, as shown in Fig. 5(b). At the 9th cycle, it reaches 137 mAh g^{-1}. However, the specific capacities of annealed LFP and LFP/C decrease from the beginning, and drop to 101 and 117 mAh g^{-1} at the 9th cycle.

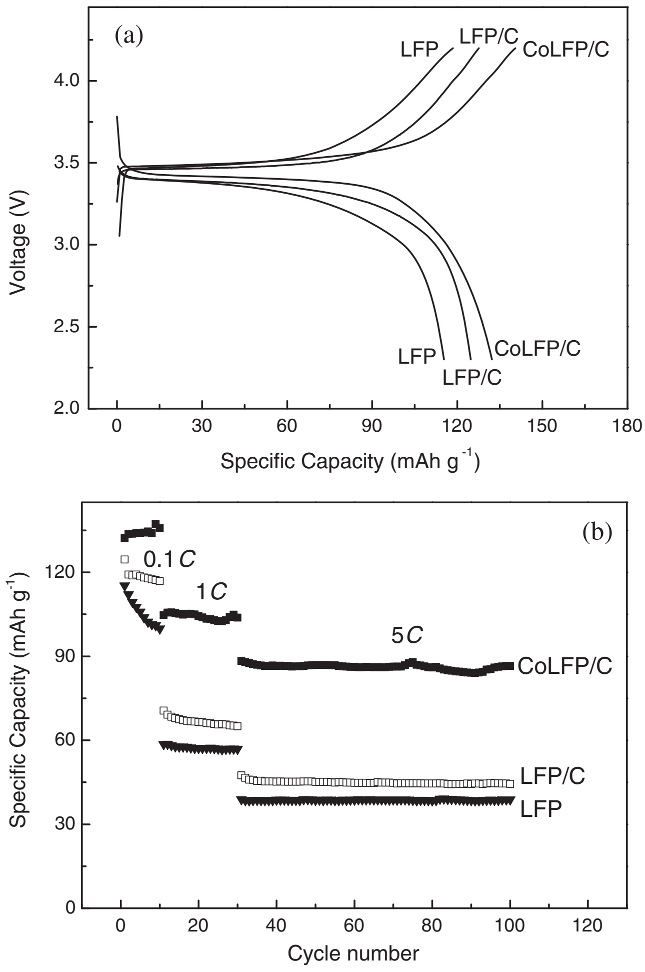

Fig. 5. The initial profiles of LFP, LFP/C and CoLFP/C after annealing between 2.3 and 4.2 V (a) and comparison of the rate performances of the three annealed samples (b).

The rate capabilities of the three annealed samples are compared in Fig. 5(b). The electrodes were cycled between 2.3 and 4.2 V at 0.1 C, 1 C, and 5 C, respectively. Not surprisingly, the annealed CoLFP/C exhibits the best rate performance. After cycling for 70 cycles at 5 C, the specific capacity of annealed CoLFP/C almost keeps unchanged and remained at 90 mAh g^{-1}. Comparatively, the capacities of annealed LFP and LFP/C decay rapidly as the rate increases, shrinking to only 39 and 45 mAh g^{-1} at 5 C. Apparently, Co-doped samples exhibit improved electrochemical properties, whether annealed or not.

As confirmed by other researchers, carbon coating can improve the performance of $LiFePO_4$, as shown in Figs. 4 and 5. The coating layer of carbon is highly graphitized, as indicated in Fig. 2, which is helpful to improve the electronic contact among particles as well as between the particles and substrates. It is interesting to point out that as Co ions were further doped in carbon-coated $LiFePO_4$, the electrochemical properties of $LiFePO_4$ can be greatly improved compared with simple carbon coating, indicating the prominent influence of Co doping.

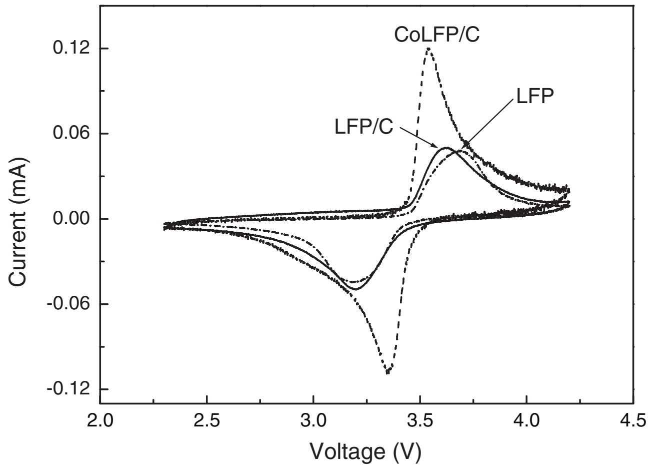

Fig. 6. Cyclic voltammograms of LFP, LFP/C and CoLFP/C.

CV measurements were conducted to explain the great improvement of electrochemical performance after Co doping. Fig. 6 presents the CV curves of LFP, LFP/C and CoLFP/C after 100 cycles at 0.1 C. For LPF and LFP/C, the oxidation peaks appear at 3.68 and 3.63 V, and the corresponding reduction peaks are centered at 3.18 and 3.20 V, respectively. The potential intervals between the redox peaks are 0.50 and 0.43 V. In comparison, the oxidation and reduction peaks are centered at 3.53 and 3.35 V for CoLFP/C with the potential interval only 0.18 V, much smaller than those of LFP and LFP/C. This implies that the polarization is effectively decreased after Co-doping. Additionally, the redox peak profile of CoLFP/C is much sharper than with LFP and LFP/C, demonstrating that the electrode reaction speed is the fastest in CoLFP/C. All these analyses show that the improved dynamic behaviors can be attributed to the Co doping.

4. Conclusion

Hydrothermal method was applied to prepare Co-doped $LiFePO_4$/C for the first time in this paper. Compared with hydrothermal prepared $LiFePO_4$/C, Co-doped $LiFePO_4$/C exhibits greatly enhanced performances. As Co ions were further doped into the carbon-coated $LiFePO_4$, the electrochemical properties were greatly improved, indicating the prominent influence of Co doping. CV characterization demonstrates that the dynamic behaviors are improved by Co doping, which partly explains the improved electrochemical performances. Based on our investigation, the great enhancement of electrochemical performance of Co-doped $LiFePO_4$/C could be attributed to the improved degree of cation order, the minimized particle size, the improved electronic contact by carbon coating and the improved electrode reaction kinetics by Co doping. Further efforts to determine the optimal preparation condition including the optimal carbon and Co contents, carbon and Co sources, synthesis and annealing conditions are under way, which will be reported in due course.

Acknowledgements

This work was supported by the National Natural Science Foundation of China (50902044 and 60976016), the Project of Cultivating Innovative Talents for Colleges & Universities of Henan Province (2002006), the Natural Science Foundation of Henan Province Department of Education (2010B480004) and Natural Science Foundation of Henan University (2008YBZR018).

References

[1] A. Padhi, K. Nanjundaswamy, J. Goodenough, J. Electrochem. Soc. 144 (1997) 1188.
[2] A. Yamada, S.C. Chung, K. Hinokuma, J. Electrochem. Soc. 148 (2001) A224.
[3] A.S. Anderesson, J.O. Thomas, J. Power Sources 97–98 (2001) 498.
[4] H.S. Kim, B.W. Cho, W.I. Cho, J. Power Sources 132 (2004) 235.
[5] M.R. Yang, W.H. Ke, S.H. Wu, J. Power Sources 146 (2005) 539.
[6] S.H. Wu, K.M. Hsiao, W.R. Liu, J. Power Sources 146 (2005) 550.
[7] S.B. Lee, I.C. Jang, H.H. Lim, V. Aravindan, H.S. Kim, Y.S. Lee, J. Alloys Compd. 491 (2010) 668.
[8] T.H. Cho, H.T. Chung, J. Power Sources 133 (2004) 272.
[9] Y. Cui, X.L. Zhao, R.S. Guo, J. Alloys Compd. 490 (2010) 236.
[10] J.F. Ni, M. Morishita, Y. Kawabe, M. Watad, N. Takeichi, T. Sakai, J. Power Sources 195 (2010) 2877.
[11] S. Shi, L. Liu, C. Ouyang, D.S. Wang, Z. Wang, L. Chen, X. Huang, Phys. Rev. B 68 (2003) 195108.
[12] D. Wang, H. Li, S. Shi, X. Huang, L. Chen, Electrochem. Acta 50 (2005) 2955.
[13] G.X. Wang, S.L. Bewlay, K. Konstantinov, H.K. Liu, S.X. Dou, J.H. Ahn, Electrochem. Acta 50 (2004) 443.
[14] M.R. Yang, W.H. Ke, S.H. Wu, J. Power Sources 165 (2007) 646.
[15] S. Franger, C. Benoit, C. Bourbon, F. Le Cras, J. Phys. Chem. Solids 67 (2006) 1338.
[16] S. Franger, F. Le Cras, C. Bourbon, H. Rouanlt, J. Power Sources 252 (2003) 119.
[17] S. Tajimi, Y. Ikeda, K. Uematsu, K. Toda, M. Sato, Solid State Ionics 175 (2004) 287.
[18] J. Lee, A.S. Teja, Mater. Lett. 60 (2006) 2105.
[19] K. Dokko, S. Koizumi, K. Sharaishi, K. Kananura, J. Power Sources 165 (2007) 656.
[20] K. Dokko, K. Shiraishi, K. Kanamura, J. Electrochem. Soc. 152 (2005) A2119.
[21] G. Meligrana, C. Gerbaldi, A. Tuel, S. Bodoardo, N. Penazzi, J. Power Sources 160 (2006) 516.
[22] J. Chen, M.S. Whittingham, Electrochem. Commun. 8 (2006) 855.
[23] J. Lee, A.S. Teja, J. Supercrit. Fluid 35 (2005) 83.
[24] T. Zhao, W.S. Chu, H.F. Zhao, X.Q. Liang, W. Xu, M.J. Yu, D.G. Xia, Z.Y. Wu, Nucl. Instrum. Method A 619 (2010) 122.
[25] Y. Cui, M. Wang, R.S. Guo, Z.H. Xu, Rare metals 28 (2009) 127.
[26] Z.Y. Tang, Y.L. Ruan, Acta Chim. Sinica 63 (2005) 1500.
[27] C.M. Burba, R. Frech, J. Electrochem. Soc. 151 (2004) A1032.
[28] K. Zaghib, A. Mauger, F. Gendron, C.M. Julien, Solid State Ionics 179 (2008) 16.
[29] B.J. Hwang, K.F. Hsu, S.K. Hu, M.Y. Cheng, T.C. Chou, S.Y. Tsay, R. Santhanam, J. Power Sources 194 (2009) 515.
[30] H. Gwon, D.H. Seo, S.W. Kim, J. Kim, K. Kang, Adv. Funct. Mater. 19 (2009) 3285.
[31] B. Kang, G. Ceder, Nature 458 (2009) 12.
[32] X.Q. Ou, G.C. Liang, J.S. Liang, S.Z. Xu, X. Zhao, Chin. Chem. Lett. 19 (2008) 345.